

Pharmacophore-based Virtual Screening: Identification of Selective Sirtuin 2 Inhibitors

Berin KARAMAN MAYACK^{1, 2, 3, *} , Muhammed Moyasar ALAYOUBI⁴ 

¹ Department of Pharmacology, School of Medicine, University of California, Davis, Davis, CA, United States.

² Department of Pharmaceutical Chemistry, Faculty of Pharmacy, Istanbul University, Istanbul 34116, Türkiye.

³ Department of Pharmaceutical Chemistry, Faculty of Pharmacy, Biruni University, Istanbul 34010, Türkiye.

⁴ Faculty of Engineering and Natural Sciences, Sabanci University, Istanbul 34956, Türkiye.

* Corresponding Author. E-mail: bkaramanmayack@ucdavis.edu, karaman.berin@gmail.com (B.K.M.); Tel. +01-916-305 99 41.

Received: 12 April 2023 / Revised: 02 June 2023 / Accepted: 03 June 2023

ABSTRACT: The Class III histone deacetylases protein Sirt2 has been implicated in the pathogenesis of several age-related diseases such as inflammation, cancer, and type II diabetes and is considered an attractive novel therapeutic target. High-quality small-molecule inhibitors of Sirt2 are vital as chemical probes for target validation and potential starting points for new therapeutics. We applied an iterative virtual screening campaign including structure-based pharmacophore generation, ensemble docking, and protein-ligand interaction fingerprint analysis, to identify potential Sirt2 inhibitors from commercially available chemical libraries. Several hit molecules were determined to make exceptional interactions both with the catalytic (C) pocket and selective extended C pocket (EXC) pocket at the same time which indicated that these compounds represent promising lead structures for the development of selective and potent Sirt2 inhibitors.

KEYWORDS: Sirt2; virtual screening; pharmacophore; molecular docking; drug discovery.

1. INTRODUCTION

Sirtuins are NAD⁺-dependent Class III histone deacetylases (HDAC) that are homologous to the yeast silent information regulator 2 (Sir2) gene [1]. Among the human sirtuin isoforms (Sirt1-7), Sirt2 is the only sirtuin protein that actively shuttles between the nucleus and cytoplasm but also can be found in the mitochondria [2]. Therefore, growing evidence has shown that Sirt2 has multifaceted functions in aging and age-related diseases such as Parkinson's disease, inflammation, cancer, and metabolic syndromes such as type II diabetes [3]. Understanding the role of Sirt2 in clinical disorders depends on the availability of chemical probes with physicochemical properties, isoform-specific, and drug candidates that can be used in biological tests. Until today several Sirt2 modulators have been disclosed in the literature. However, most of these compounds lack potency, isotype selectivity, or drug-like pharmacokinetic properties which hampers their use in physiological studies of Sirt2 or as a potential drug to combat Sirt2-linked pathologies.

Recently, two identical indole-derived molecules were found to bind Sirt2 protein, one onto the catalytic pocket (C pocket) and the other one onto the selective pocket (extended C pocket; EXC) (Figure 1) [4]. These ligands have been found to induce approximately ~6 Å displacement in the hinge region [5]. These findings showed that the Sirt2 protein was more flexible in the hinge region than the close homologous proteins Sirt1 and Sirt3 isoforms and that it can obtain different conformations depending on the ligand type. Thus, these structures provide a good starting point for the structure-based design of novel selective Sirt2 inhibitors. In this study, we aim to identify novel molecules that could interact with both the C and EXC pockets of Sirt2 at the same time and show similar binding interactions seen for the indole-derived inhibitors, Ex-243 and CHIC35. As all the important pharmacophore groups will be collected in one molecule, we hypothesize that these new molecules would be more active and selective than the already published modulators of Sirt2 in the literature.

Molecular modeling techniques encompass both theoretical and computational methods to generate, represent and manipulate molecular systems ranging from small organic compounds to large biomolecules.

How to cite this article: Karaman Mayack B, Alayoubi MM. Pharmacophore-based Virtual Screening: Identification of Selective Sirtuin 2 Inhibitors. J Res Pharm. 2023; 27(4): 1366-1379.

Computer-aided approaches have been heavily used in the drug design and development field and their successful applications have accelerated the discovery of several drugs at a significantly lower cost [6].

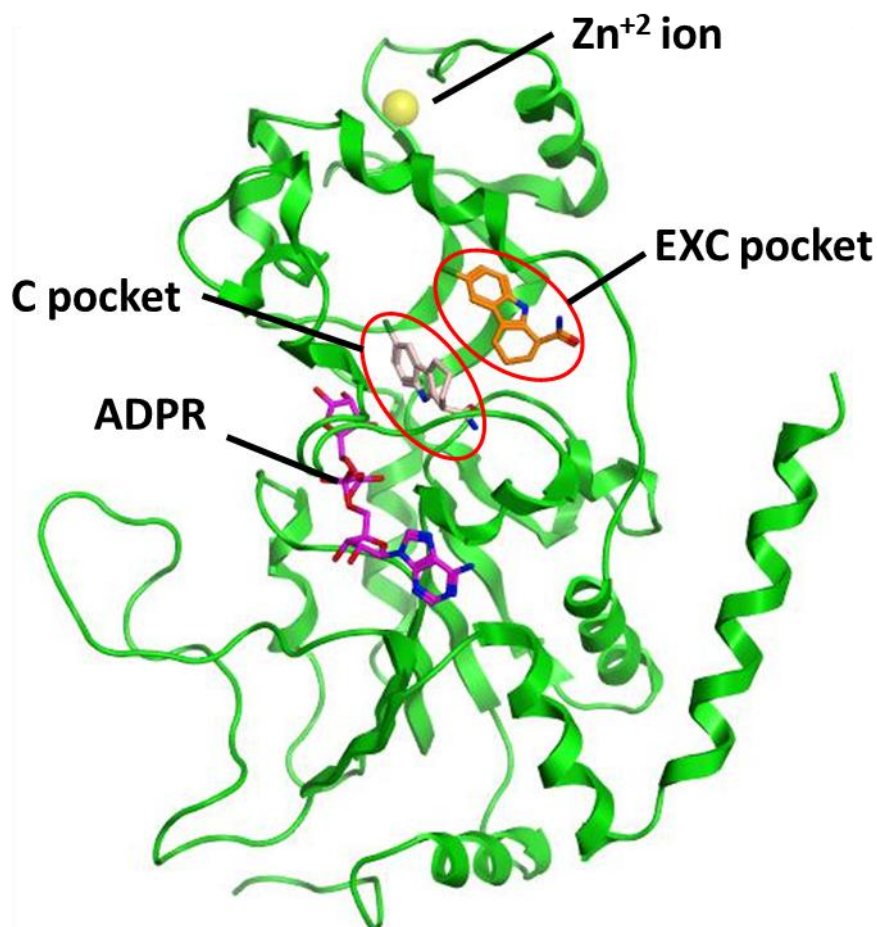


Figure 1. Crystal structure of the human isoform Sirt2 (green ribbon) in complex with Ex-243 (C pocket; light pink sticks, EXC pocket; orange sticks) and ADPR substrate analog (dark pink sticks) (5D7P.pdb) [4]. Zn²⁺ ion is represented as a yellow sphere.

One of the widely used *in silico* drug design tools is molecular docking which predicts the binding mode of a given molecule to its macromolecular target [7]. Most often docking studies are performed on a single static target crystal structure or a comparative model keeping the ligand flexible. However, it is known that ligand binding induces important conformational changes in proteins and that one experimentally derived structure represents only one conformational substate out of a protein's high dimension and unevenly populated conformation space. Although there are successful examples of the correct determination of the ligand binding mode, based on a single structure approach, docking accuracy can drop off dramatically using structures with no ligand-bound or with those in complex to very different ligands. Moreover, incorporating target flexibility has been demonstrated to improve new hit identification, pose prediction, as well as binding affinity estimation [8]. To incorporate protein flexibility in docking, different approaches have been investigated. One of the widely used methods is called ensemble docking in which an ensemble of target conformations coming from either X-ray crystallography or NMR spectroscopy is used for docking experiments [9].

Another computational tool that is extensively used in structure-based drug research is the application of the pharmacophore concept [10]. International Union of Pure and Applied Chemistry defines a pharmacophore model as 'an ensemble of steric and electronic features that is necessary to ensure the optimal supramolecular interactions with a specific biological target and to trigger (or block) its biological response' [11]. There are two main strategies to construct a pharmacophore model: (1) structure-based pharmacophore modeling and (2) ligand-based pharmacophore modeling [12]. Receptor-based or so-called structure-based receptor modeling relies on the 3D structure of the target and the identification of important interaction points

probed from available ligand-protein complexes or mutation studies. On the other hand, ligand-based pharmacophore modeling depends on the availability of known active molecules to attain the shared common features that are important for biological activity. In order to develop reliable pharmacophore models, validation of these models with a training set (and if available enriching these sets with inactive molecules, weak binders, or decoy molecules) is essential. Moreover, a good sampling of the conformational space both for the training compounds and the virtual libraries that will be screened is critical.

In the present work, a series of computer-aided drug discovery approaches including ensemble docking, database filtering, and pharmacophore-based virtual screening was applied to identify potential Sirt2 selective inhibitors from commercial small molecule libraries. Primarily, we generated several pharmacophore models using a combination of different features based on the recently resolved crystal structures of Sirt2-indole-derived inhibitors. Subsequently, these models were used to filter commercial libraries. Next, we carried out ensemble docking experiments on the filtered molecules and top-ranked compounds were post-processed according to Lipinski's Rule of Five (Ro5) [13]. Finally, the structural protein-ligand interaction fingerprints were used to select the hit molecules that favor the similar interactions seen for Sirt2 inhibitors, Ex-243 and CHIC35.

2. RESULTS and DISCUSSION

2.1 Validation of Molecular Docking Protocol

Molecular docking is one of the main techniques used to predict the interactions and/or biological activity of compounds with the active site of the target protein. Therefore, docking programs generally have two applications; (1) to identify key molecular recognition motifs by pose estimation and (2) to estimate relative binding free energy to distinguish between active and inactive molecules in virtual scanning [14,15]. As already shown in many studies in the literature, the top-scored pose is not always the closest to the experimental one [15-18]. A docking solution with an RMSD value of less than 2.0 Å between the heavy atoms of the experimental pose and the predicted *in silico* pose has been widely accepted as a successful docking pose [19,20]. However, some studies such as cross-docking or self-docking analysis of large ligands have used 2.5 Å as a threshold value for their RMSD analysis [21]. In such studies, an average of 70% of the highest-scoring poses have been found to have an RMSD of 2.0 Å or less between the native pose and the docking solution [20].

In this study, the pose estimation power of the XP and SP scoring functions and the ranking accuracy of both dockingscore and emodel score of the GLIDE program implemented on the Schrödinger Platform (Schrödinger Version 2019: LigPrep, Schrödinger, LLC, New York, NY, 2019) was evaluated [22-24]. For this, the indole-inhibitors CHIC35, an analog of Ex-527, (Sirt2-ADPR-CHIC35 complex; 5D7Q.pdb) and Ex-243 (Sirt2-ADPR-Ex243 complex; 5D7P.pdb) were redocked and the RMSD value between the produced poses and the crystal poses was calculated (Table S1-5). Since the hinge loop in the EXC pocket adopts a different conformation in the A and B chains of both Sirt2-indole inhibitor complexes, all four crystal structures were included in our docking studies. An RMSD value of less than 2.0 Å was accepted as a threshold for an 'acceptable' docking solution. The ligands were re-docked onto complexes with and without bridging waters to determine the docking accuracy. A docking accuracy of 38%, 62%, 77%, and 77% were obtained for the XP-dockingscore, SP-dockingscore, XP-emodel score, and SP-emodel score, respectively (Figure S1-5). Although the XP mode was designed to filter out false positive poses and improve the correlation between good poses and good scores, in the present study, it did not show a significant superiority over SP mode in terms of docking accuracy. Also, XP mode requires a significant amount of CPU time, and docking a large number of molecules is time-consuming with this scoring function. Thus, for ensemble docking of virtual compound libraries, instead of twenty poses, for each ligand, we generated ten poses for the post-minimization step and then, the pose with the highest SP-emodel score was selected for further analysis.

1.2. Structure-based Pharmacophore Model Generation

In the present work, we aimed to identify compounds that could bind both to the catalytic (C) pocket, as well as to the recently identified selective extended C pocket (EXC) of the Sirt2 protein. The idea behind this work is to identify hits that target key interactions in both C and EXC pockets at the same time. Thus, we aimed to identify ligands that consist of features important for Sirt2 inhibitory activity but at the same time bear components responsible for the isoform selectivity. Therefore, we used the two recently solved crystal

structures of Sirt2 with low μM indole inhibitors, EX-243 and CHIC35, for our structure-based pharmacophore modeling campaigns.

A typical macromolecule-ligand-complex-based pharmacophore modeling starts with determining the important interaction points between the ligand and the protein, and their spatial relationships. Next, the selected chemical features are assembled in a structure-based pharmacophore model. Finally, in the presence of a set of both active and inactive compounds, pharmacophore models are validated and the one with the highest selectivity power is chosen for virtual screening experiments. However, compounds bind at the same time both to the C and EXC pockets of Sirt2 and mimic similar interactions as the co-crystallized indole inhibitors have not been found in the literature. To overcome this problem, Robaa et al. proposed screening large molecule libraries using multiple pharmacophore models instead of a single validated consensus pharmacophore model [25]. This method has shown to be successful in cases where active molecules are missing, and the pharmacophore model cannot be validated. This method was also adapted in the present work.

First, we used the Pharmacophore Consensus tool implemented in Molecular Operating Environment (MOE) software [26] to generate pharmacophore annotation points on both ligands observed in the Sirt2-ADPR-CHIC35 and Sirt2-ADPR-EX243 crystal complexes in C and EXC pockets (Figure 2). The resulting common model shown in Figure 2c is characterized by 22 features automatically created on the aligned ligands. The common pharmacophore model includes 6 aromatic features and 6 hydrophobic features occupied by the carbazole ring of EX-243, the cyclohepta[b]indole ring of CHIC35, and the chlorine atom. Moreover, the pharmacophore query consists of seven hydrogen bond acceptors between the amide carbonyl of the ligands and the sidechains of Ile169 and Asp170 residues in the C pocket and the bridging water molecule in the EXC pocket. In addition, the model contains three hydrogen bond donors between the NH_2 of the amide group of ligands and the bridging water molecule and Asp170 residue in the C and pocket and Leu138 and Gly141 residues in the EXC pocket.

Next, based on the protein-ligand interactions observed in the crystal structures (Figure 3-4), we generated four different pharmacophore queries (**EHT2 a-d**, Figure 5) using different combinations of the suggested set of features (Figure 2c).

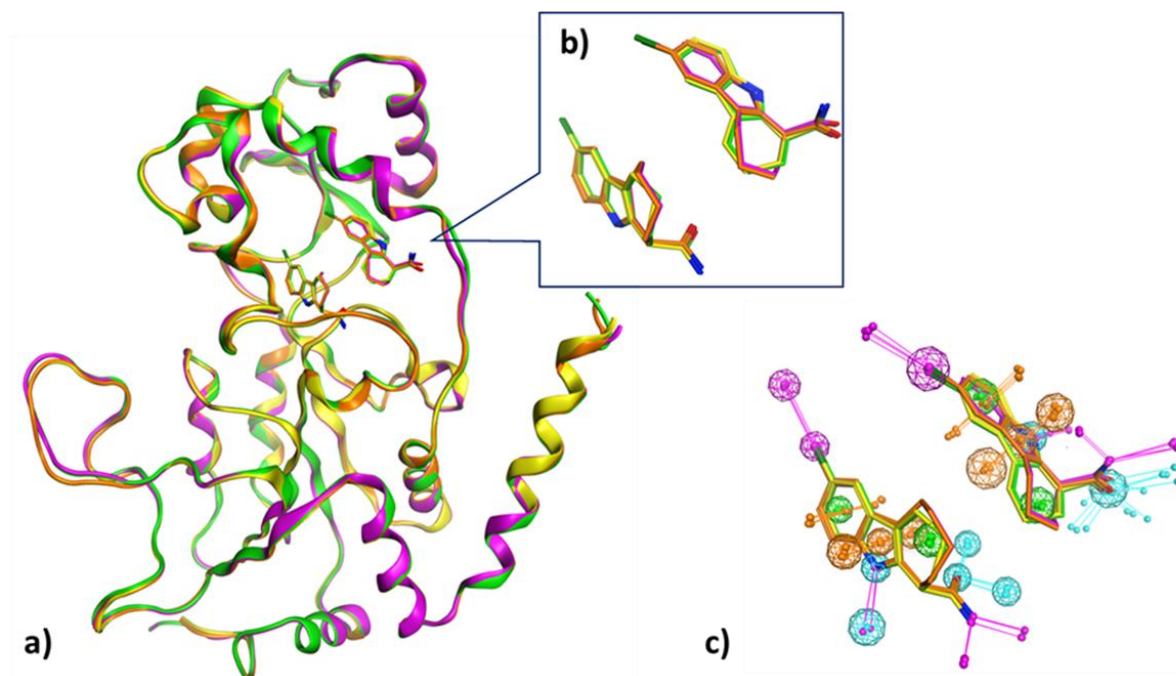
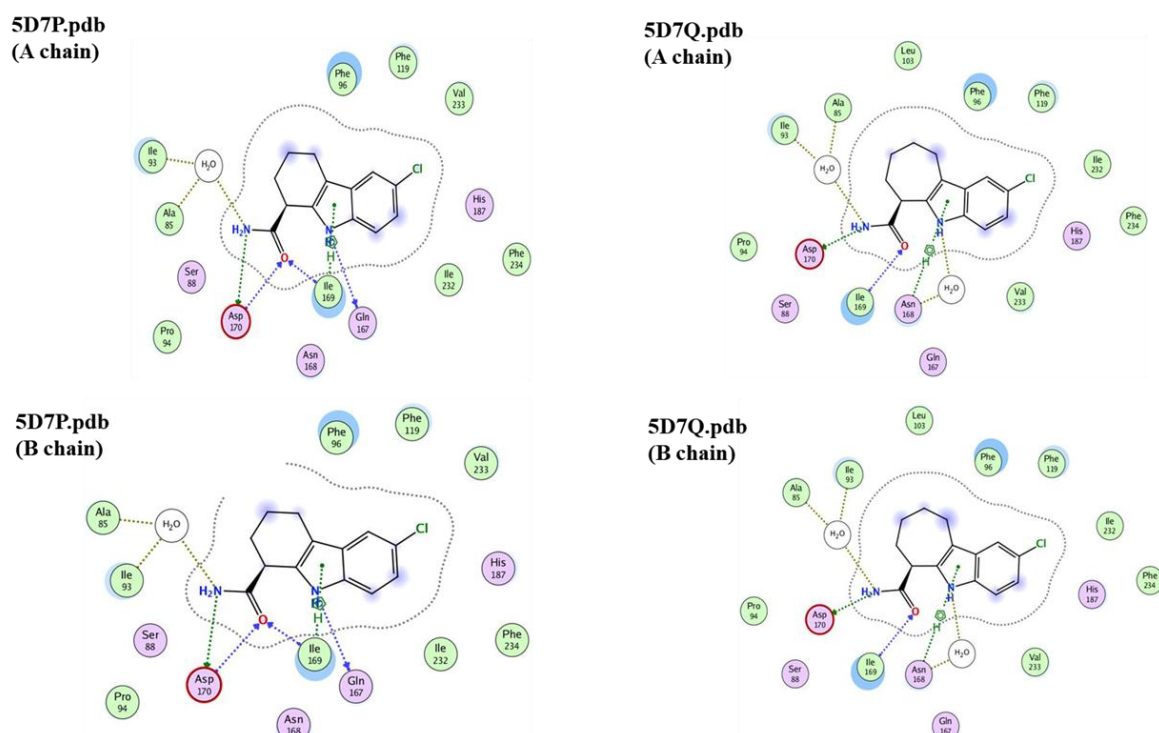


Figure 2. Structure-based pharmacophore model generation. a) Superimposed crystal structures of 5D7P.pdb A chain (green), 5D7P.pdb B chain (yellow), 5D7Q.pdb A chain (pink), and 5D7Q.pdb B chain (orange) is shown as line models and the co-crystallized ligands belonging to each chain are shown as sticks with the respective color belonging to the chain. b) Close up view of the co-crystallized ligands Ex-243 (PDB ID: OCZ) in 5D7P.pdb A and B chains and CHIC35 (PDB ID: 4I5) in 5D7Q.pdb A and B chains c)

Pharmacophore annotation points automatically created on ligands using the Pharmacophore Consensus tool implemented in MOE. Pink, turquoise, green, and orange dots and spheres represent H-bond donor, H-bond acceptor, hydrophobic, and aromatic chemical functionalities, respectively.



C pocket

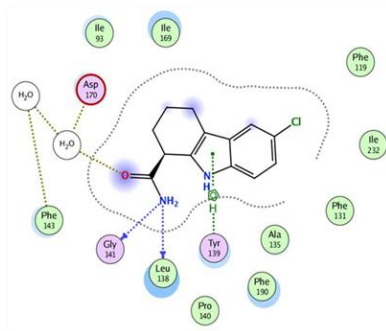
Figure 3. 2D interaction diagram of co-crystallized ligands in the catalytic (C) pocket of Sirt2–ADPR–EX243 (5D7P.pdb) and Sirt2–ADPR–CHIC35 (5D7Q.pdb) complexes

1.3. Virtual Screening of Commercial Databases

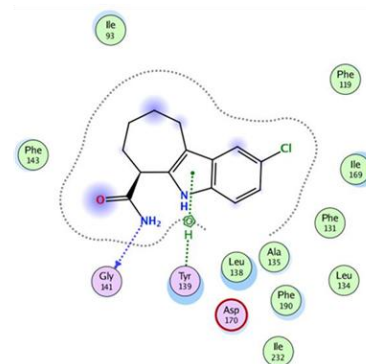
Before performing a pharmacophore-based virtual screening campaign on the selected commercial libraries, we pre-filtered them to eliminate the undesirable compounds that appear as frequent hitters in several biochemical high throughput experiments by applying (pan-assay interference compounds) PAINS substructure filter [27] and to identify only lead-like small molecules by employing (Rapid Elimination of Swill) REOS rules [28]. The number of molecules present in the original library, after preparation with the LigPrep module in Schrödinger software and upon pre-filtering by PAINS and REOS rules available in the Canvas-Schrodinger tool is presented in Table S6.

Subsequently, the performance of the four pharmacophore queries, **EHT2 a-d**, was tested on the three subsets, BioDesign Library, Elites & Synergy Libraries, and Gold & Platinum Collections of Asinex database [29]. The number of molecules retrieved as hits upon pharmacophore-based virtual screening (PBVS) of the Asinex database is presented in Table 1. Due to the low selectivity power of the **EHT2b** and **EHT2c** pharmacophore models, the **EHT2a** and **EHT2d** pharmacophore models were selected for PBVS of Chembridge [30], ChemDiv [31], and Enamine [32] molecule libraries. Molecules obtained after the PBVS search were subjected to three consecutive post-filtering processes.

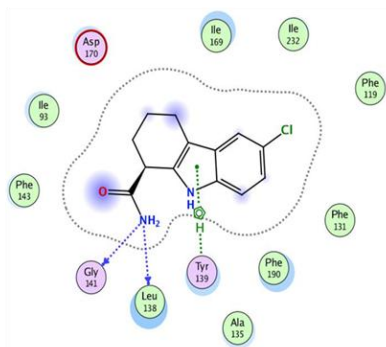
5D7P.pdb
(A chain)



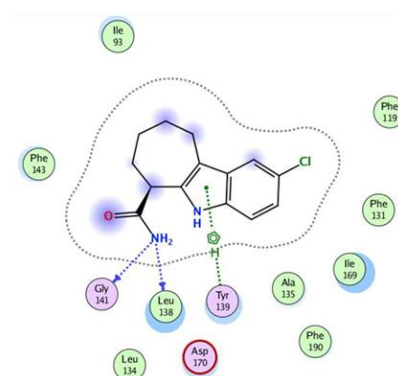
5D7Q.pdb
(A chain)



5D7P.pdb
(B chain)



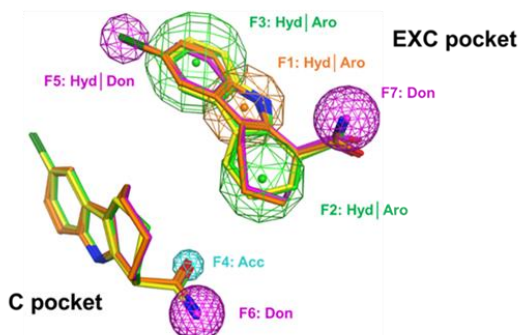
5D7Q.pdb
(B chain)



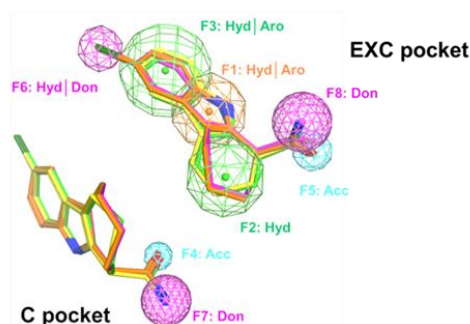
EXC pocket

Figure 4. 2D interaction diagram of co-crystallized ligands in the extended C (EXC) pocket of Sirt2-ADPR-EX243 (5D7P.pdb) and Sirt2-ADPR-CHIC35 (5D7Q.pdb) complexes

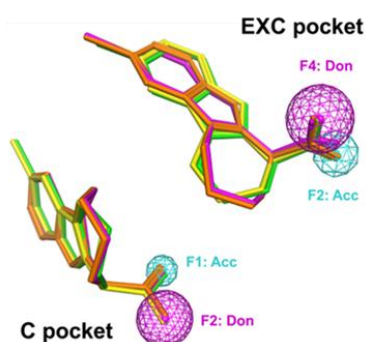
EHT2a



EHT2b



EHT2c



EHT2d

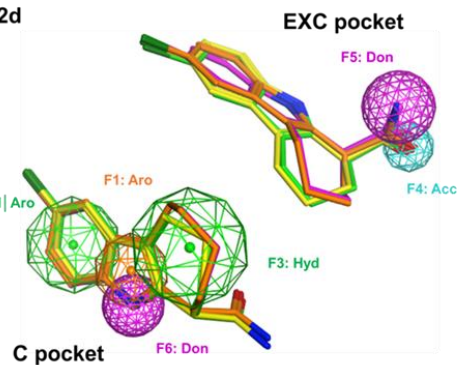


Figure 5. 2D interaction diagram of co-crystallized ligands in the extended C (EXC) pocket of Sirt2-ADPR-EX243 (5D7P.pdb) and Sirt2-ADPR-CHIC35 (5D7Q.pdb) complexes

Table 1. Pharmacophore-based virtual screening results for Asinex database subsets

Pharmacophore	Asinex Screening Database Subsets		
Model	BioDesign	Elite & Synergy	Gold & Platinum
EHT2a	531	187	160
EHT2b	144,857	71,541	88,809
EHT2c	118,629	5,625	71,282
EHT2d	4569	1793	548

Molecular docking, which is widely used in structure-based virtual screening studies, was chosen as the first post-filtering method. When we visually examined the crystal complexes Sirt2-ADPR-EX243 (5D7P.pdb) and Sirt2-ADPR-CHIC35 (5D7Q.pdb), we realized that Phe190 and TYR139 residues adopted different conformations in different chains (data not shown). Therefore, we used both A and B chains belonging to these two complexes and thus, in total four protein-ligand complexes were used for ensemble docking studies of hit molecules coming from PBVS experiments. The docking pose with the highest SP-emodel score was used for ranking.

The ligands that ranked in the top 10% of each dataset were subjected to the second filtering step based on Lipinski's Rule of Five [13]. Accordingly, only compounds that passed the following criteria: molecular weight (MW) < 500 g/mol, hydrogen bond acceptors (HBA) ≤ 10, hydrogen bond donors (HBD) ≤ 5, and LogP ≤ 5 were selected as hits.

In the final step, the docking poses of the hit molecules were filtered according to the protein-ligand interactions observed in the crystal complexes. PLIF application [33] in the MOE program was used for this step. Thus, during the third filtration process, only molecules showing H-bond interactions between the Leu138, Gly141, Gln167, and Asp170 residues were accepted as hit molecules. In addition, compounds that form the conserved H-bond interaction seen between the Sirtuin substrates and the Val233 residue in the C pocket were also included as hits in this step [34]. In total 111, 323, 611, and 642 molecules were retrieved from PLIF analysis for ChemDiv, Asinex, Enamine, and Chembridge libraries, respectively (Table 2). Next, hit molecules were ranked based on their Ligand Efficiency (LE) score obtained by dividing the docking score (DS; SP emodel score) by the number of heavy atoms of that ligand. The chemical structures, DS and LE scores, and some of the 2D properties of hit molecules ranked in the top ten are presented in Figure 6. It is important to note that all the top 10 hits were coming from the screening based on the **EHT2d** pharmacophore model.

When we visually analyzed the protein-ligand interactions of the top 10 hits, all the compounds except **hit 5** make interactions with residues located both in C and EXC pockets. Since we would like to find compounds that can bind into these two pockets at the same time, top-hit molecules align well with the aim of this study. All the hits except **hit 8** make H-bond interactions with Ile169 in the C pocket. Moreover, the second most seen interaction was with another residue in pocket C, Asp170. All hit molecules except **hits 1** and **10** were favoring an H-bond interaction with or without a water bridge with the residue Asp170. We have also seen additional water bridging H-bond interactions between the residue Ala85 and **hits 2, 4, 5, and 6**, between the residue Ile93 and **hits 2, 4, and 9**, and between Pro94 and **hit 9**. Furthermore, residue Asn168 was making direct H-bond interactions with **hits 2 and 4** and water-bridging H-bond interactions with **hit 10**. **Hit 10** was also special as it was the only hit that formed an H bond interaction with residue His187. Finally, we realized that three **hits 6, 7, and 8**, were making H-bond interactions with residue Gln167. H-bond interactions seen between the co-crystallized ligands CHIC35 and Ex243 and the EXC pocket residues Leu138 and/or Tyr139 could be captured by all the hit molecules except **5** and **9**. When we analyzed the hydrophobic interactions, pi-pi stacking interactions with residue Phe96 (all the hit molecules except **hits 2, 4, and 9**) was the most favored one. Similarly, hit molecules formed pi-pi interactions with residues Phe119 (**hits 5 and 6**), Tyr139 (**hits 1 and 2**), Phe143 (**hit 10**), His187 (**hit 10**), Phe190 (**hit 7**), and Phe235 (**hit 9**). Lastly, exclusive pi-cation interaction between Phe119 and **hit 6**, and again Tyr139 and **hits 1 and 10** were observed.

Table 2. Summary of the screening results obtained for different commercial vendors in this study.

Pharmacophore Model	Asinex ²⁴				ChemBridge ²⁵			
	PBVS	ED	Ro5	PLIF	PBVS	ED	Ro5	PLIF
EHT2a	878	87	49	31	1458	144	126	72
EHT2d	6910	688	348	292	9784	976	819	570
	ChemDiv ²⁶				Enamine ²⁷			
	PBVS	ED	Ro5	PLIF	PBVS	ED	Ro5	PLIF
EHT2a	1094	106	21	14	365	36	28	17
EHT2d	3569	354	161	97	11826	1181	1074	594

3. CONCLUSION

The current study aimed to identify novel and selective inhibitors of the Sirt2 isoform using structure-based drug discovery approaches including pharmacophore-based virtual screening and 3 subsequent post-filtering methods; molecular docking, 2D chemical properties, and protein-ligand interaction fingerprint analysis. Structure-based pharmacophore model was built based on indole-like inhibitors, CHIC35 and Ex-243, of Sirt2 that were shown to bind both in C and selective EXC pockets. The generated pharmacophore model was used for screening different commercial screening libraries consisting of Asinex, ChemBridge, ChemDiv, and Enamine virtual screening databases. A significant number of virtual “hits” have been identified from these libraries which were further post-filtered as aforementioned. Hits were further ranked based on their ligand efficiency scores before visual analysis. The top 10 hits showed similar key interactions seen for the co-crystallized ligands, CHIC35 and Ex-243, with Sirt2. Since the hit molecules make exceptional interactions both with C and EXC pockets at the same time, they represent reasonable starting compounds for the identification of selective and potent novel lead structures against Sirt2.

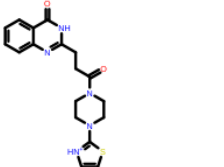
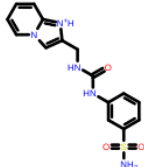
4. MATERIALS AND METHODS

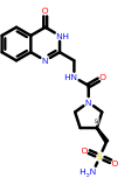
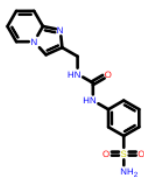
4.1. Preparation of Virtual Libraries

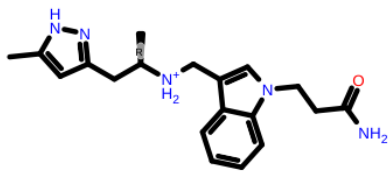
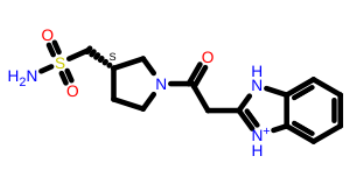
Asinex [29], ChemBridge [30], ChemDiv [31], and Enamine [32] screening libraries were downloaded from the companies’ websites. Ligands were prepared using the LigPrep tool. The possible ionization degrees of the molecules at pH 7.0 ± 2.0 were produced. Specified chirality was retained and other chiral centers were varied with a maximum of 32 possible stereoisomers. Low-energy 3D structures of the compounds were obtained using the Optimized Potentials for Liquid Simulations (OPLS) force field OPLS3e. All other parameters for ligand preparation were kept as the default. Compounds in databases that may cause false positive results during biological activity assays (PAINS, pan assay interference compounds) [27], and that carry reactive functional groups (Rapid Elimination of Swill, REOS) [28] were filtered using the Schrödinger-Canvas module (Table S6). Conformation production was carried out using the OMEGA tool [35] and a maximum of 400 different conformers of each molecule was prepared.

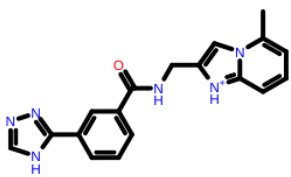
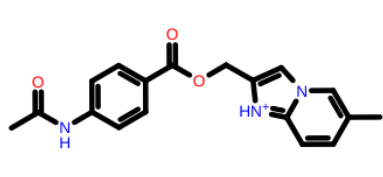
4.2. Preparation of protein-inhibitor complexes

X-ray structures of Sirt2 protein in complex with cofactor ADPR (adenosine diphosphate ribose) and indole-inhibitors CHIC35 (Sirt2-ADPR-CHIC35 complex; 5D7Q.pdb) and Ex-243 (Sirt2-ADPR-EX243 complex; 5D7P.pdb) were prepared (Figure S1). The .pdb files of the complexes were taken from the Protein Data Bank. The complexes were split into single chains and each chain was prepared using Schrodinger's Protein Preparation Wizard module. In summary, hydrogen atoms were added, appropriate bond orders were assigned, and C and N terminals were capped with *N*-acetyl and *N*-methyl amide groups. The orientations of the water molecules were sampled, and the H-bond network was optimized using Propka at pH = 7.0. Then, to eliminate steric conflicts, energy minimization of the complexes was carried out using the OPLS3e force field and a termination criterion of 0.3 Å Root Mean Square Deviation (RMSD) of heavy atoms.

			
Docking Score	-12.779	Docking Score	-11.438
LE	-0.491	LE	-0.477
a_heavy	26	a_heavy	24
Weight	370.457	Weight	346.391
a_acc	3	a_acc	3
a_don	1	a_don	3
b_rotN	5	b_rotN	6
logP(o/w)	1.001	logP(o/w)	0.452
database	Enamine	database	Enamine

			
Docking Score	-11.79	Docking Score	-10.945
LE	-0.472	LE	-0.456
a_heavy	25	a_heavy	24
Weight	365.414	Weight	345.383
a_acc	5	a_acc	4
a_don	3	a_don	3
b_rotN	6	b_rotN	6
logP(o/w)	-1.348	logP(o/w)	-0.098
database	chembridge	database	Enamine

			
Docking Score	-11.322	Docking Score	-9.929
LE	-0.453	LE	-0.451
a_heavy	25	a_heavy	22
Weight	340.451	Weight	323.397
a_acc	3	a_acc	3
a_don	3	a_don	1
b_rotN	8	b_rotN	5
logP(o/w)	2.493	logP(o/w)	0.223
database	chembridge	database	chembridge

			
Docking Score	-11.161	Docking Score	-10.703
LE	-0.446	LE	-0.446
a_heavy	25	a_heavy	24
Weight	333.375	Weight	324.36
a_acc	4	a_acc	2
a_don	4	a_don	1
b_rotN	5	b_rotN	6
logP(o/w)	2.716	logP(o/w)	2.328
database	Enamine	database	Enamine

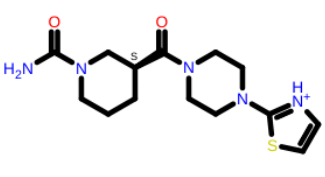
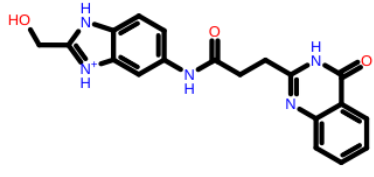
			
Docking Score	-9.683	Docking Score	-11.783
LE	-0.44	LE	-0.436
a_heavy	22	a_heavy	27
Weight	324.429	Weight	364.385
a_acc	2	a_acc	4
a_don	1	a_don	2
b_rotN	4	b_rotN	6
logP(o/w)	-0.461	logP(o/w)	1.229
database	chembridge	database	Chemdiv

Figure 6. The chemical structures predicted scores and some of the 2D properties of the top ten hit molecules. Hits are ranked based on their LE score from left to right and top to bottom.

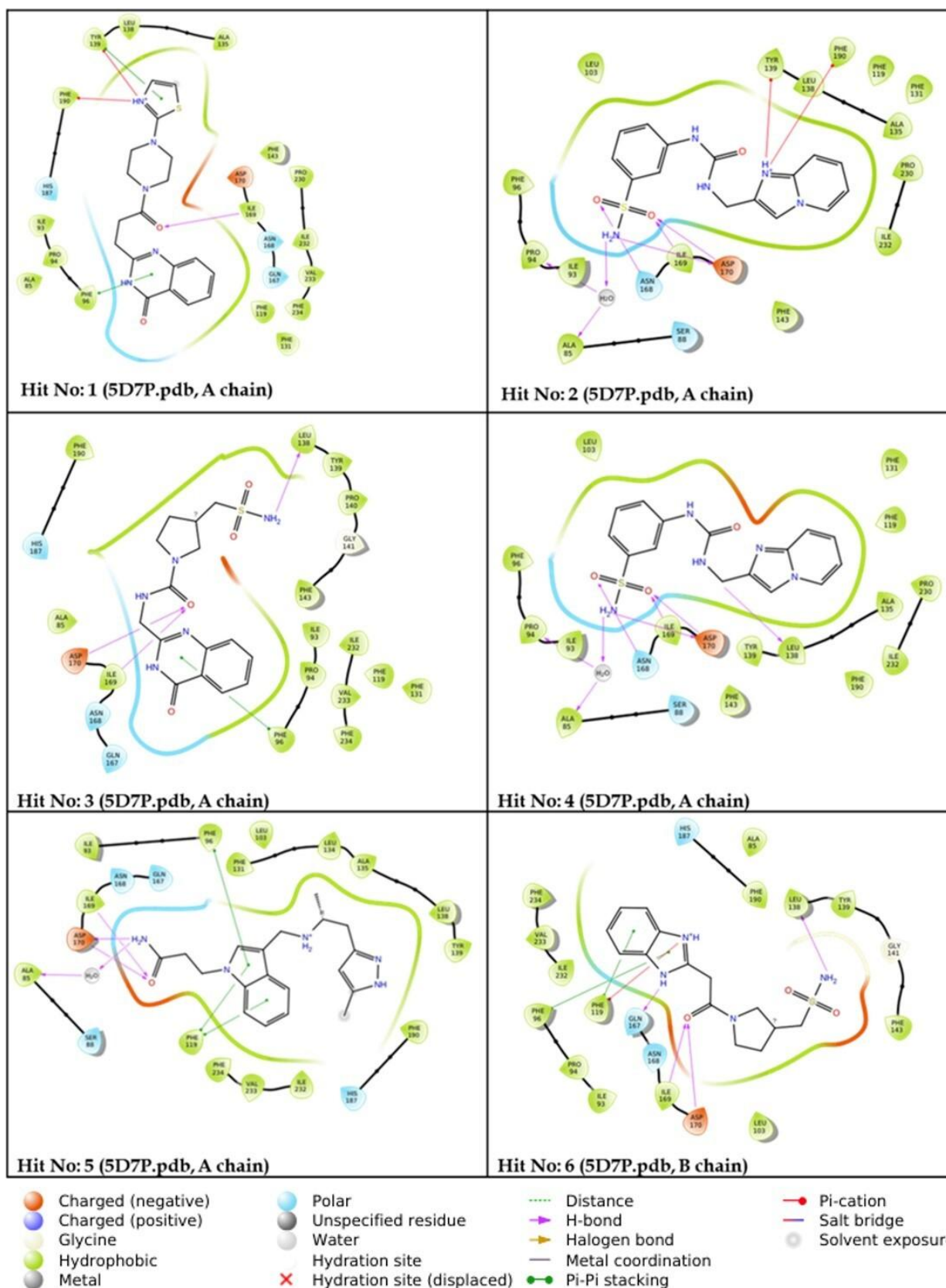


Figure 7. 2D interaction diagram of the top 10 hit molecules with the corresponding protein structure

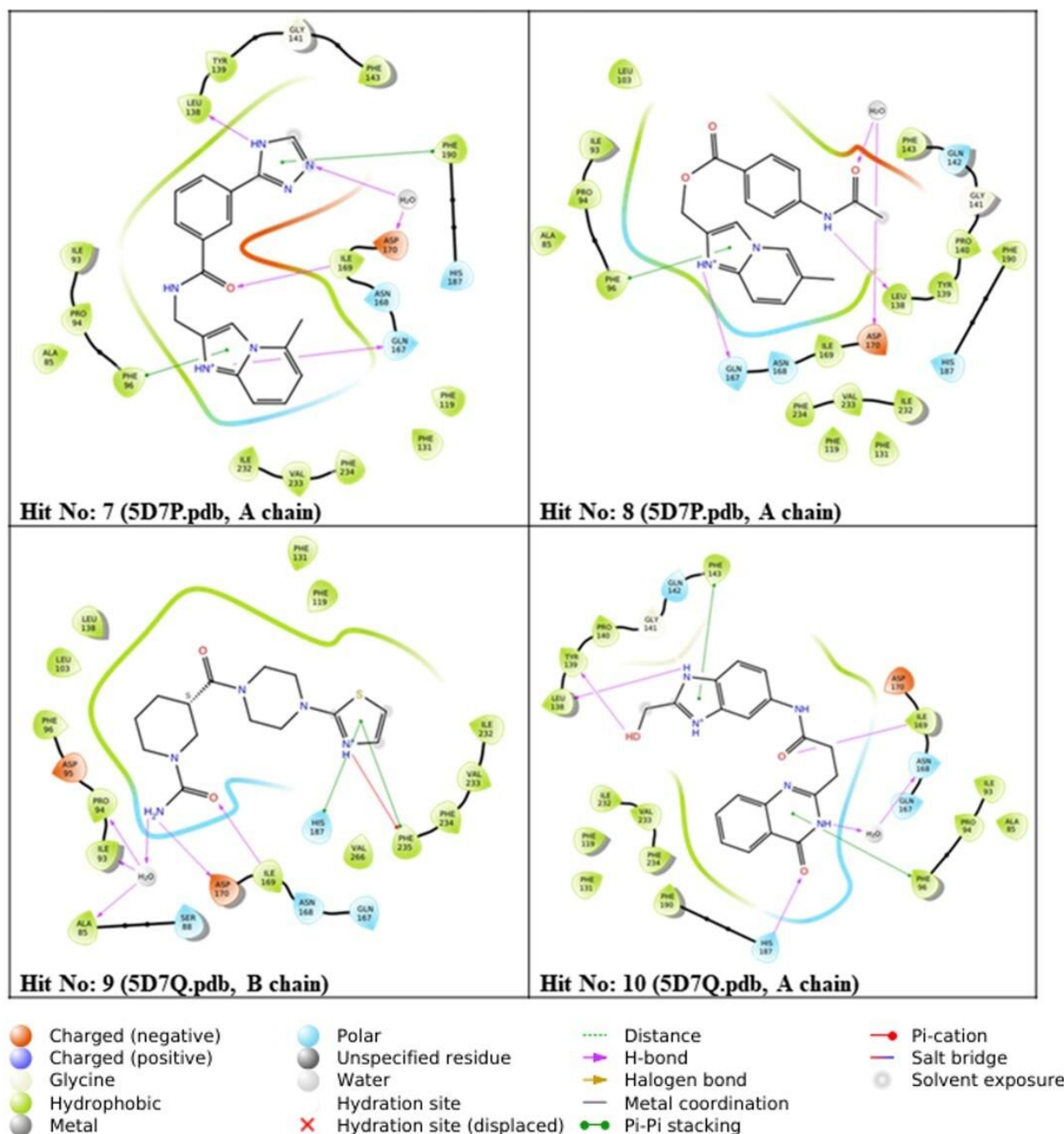


Figure 7. (Continued).

All water molecules except the bridging water molecules found in the crystal structure of the Sirt2-ADPR-CHIC35 complex (A chain: HOH513 and HOH557, B chain: HOH502 and HOH529) and Sirt2-ADPR-EX243 complex (A chain: HOH545, HOH551, HOH558, and HOH641, B chain: HOH504 and HOH569) were deleted.

4.3. Molecular Docking

Blind docking experiments were conducted using the Glide docking tool implemented in Schrödinger. Both Standard Precision (SP) and extra precision (XP) scoring functions were used for self-docking analysis. While creating the grid files, all combinations were considered by using protein-ligand complexes that contain both bridging water molecules and no water molecules. The position of the co-crystallized inhibitor in the crystal structures was used to define the binding site. A total of 20 poses were kept for post-minimization and a maximum of 10 top-scored poses were saved. The top-scored pose was evaluated for RMSD calculations.

4.4. Structure-based Pharmacophore Model Generation

The development of pharmacophore models was carried out using the Pharmacophore Query Editor tool implemented in the MOE program. We first superimposed the chains of the Sirt2-ADPR-CHIC35 complex (5D7Q.pdb) and Sirt2-ADPR-EX243 complex (5D7P.pdb) using the Protein Align/Superpose application in the MOE program. Then, the Pharmacophore Consensus option was used to generate suggested features for the pharmacophore queries based on the Extended Hückel Theory (EHT) pharmacophore scheme. With this method, a certain energy threshold (determined in kcal/mol) needs to be overcome for an H-bond interaction to form. This energy is calculated by a “receptor strength multiplier” and the power of the interacting atom pair. “Acc >” defines the minimum strength of the acceptor atom and the projected acceptor annotation point to be interacted with, and “Don >” indicates the minimum strength of the donor atom and the projected donor annotation point to be interacted with.

Based on the protein-ligand interactions observed in the crystal complexes, four pharmacophore models, **EHT2 a-d**, were created (**Figure 5**). The **EHT2a** pharmacophore query consists of 7 pharmacophoric features (F1-7). F1, F4, F6, and F7 were set as mandatory features. Moreover, among F2, F3, and F5 features of the query were marked as “at least one of them must be matched to its projected feature”. In addition, for F4, F5, F6, and F7 features, we set the strength of the interacting atom to be Acc>0.48, Don>1, Don>0.33, and Don>0.5, respectively. In the **EHT2b** model, there were 8 pharmacophore features in total. F4 and F7 features were set as mandatory features to be matched. Besides, at least two of the F1, F2, F3, and F6 pharmacophore features were required to be matched, and at least one of the F5 and F8 pharmacophore groups had to be matched. Furthermore, for the F4, F6, F7, and F8 features, the strength of the atom to be interacted with was set to Acc>0.48, Don>1, Don>0.33, and Don>0.5, respectively. The **EHT2c** pharmacophore query contains a total of 4 pharmacophoric features (F1-4). All features were set as mandatory. In addition, for F1-4 features pharmacophore groups, we set the strength of the interacting atom to be Acc>0.48, Acc>1, Don>0.33, and Don>0.5, respectively. In the **EHT2d** model, there were a total of 6 features (F1-6). F4, F5, and F6 pharmacophoric features were set as mandatory. Moreover, at least two of the F1, F2, and F3 pharmacophore groups were required to be matched. Additionally, for features, F4, F5, and F6, we set the strength of the interacting atom to be Acc>1, Don>0.5, and Don>0.5, respectively.

This is an open access article which is publicly available on our journal's website under Institutional Repository at <http://dspace.marmara.edu.tr>.

Acknowledgements: This work was supported by Biruni University Scientific Research Coordination Unit. Project Number: Biruni-Bap-2019-01-14. The authors would like to give acknowledgments to the Department of Pharmaceutical Chemistry, Faculty of Pharmacy, Istanbul University.

Author contributions: B.K.M. designed the study and wrote the paper. B.K.M. and M.M.A. performed computational analysis. All authors read and commented on the manuscript.

Conflict of interest statement: The authors declare no conflict of interest.

REFERENCES

- [1] Baur JA, Ungvari Z, Minor RK, Le Couteur DG, de Cabo R. Are sirtuins viable targets for improving healthspan and lifespan? *Nat Rev Drug Discov*. 2012; 11(6): 443-461. <https://doi.org/10.1038/nrd3738>.
- [2] Houtkooper RH, Pirinen E, Auwerx J. Sirtuins as regulators of metabolism and healthspan. *Nat Rev Mol Cell Biol*. 2012; 13(4): 225-238. <https://doi.org/10.1038/nrm3293>.
- [3] Wang Y, Yang J, Hong T, Chen X, Cui L. SIRT2: Controversy and multiple roles in disease and physiology. *Ageing Res Rev*. 2019;55:100961. <https://doi.org/10.1016/j.arr.2019.100961>.
- [4] Rumpf T, Gerhardt S, Einsle O, Jung M. Seeding for sirtuins: microseed matrix seeding to obtain crystals of human Sirt3 and Sirt2 suitable for soaking. *Acta Crystallogr F Struct Biol Commun*. 2015;71(Pt 12):1498-1510. <https://doi.org/10.1107/s2053230x15019986>.
- [5] Schiedel M, Robaa D, Rumpf T, Sippl W, Jung M. The Current State of NAD⁺-Dependent Histone Deacetylases (Sirtuins) as Novel Therapeutic Targets. *Med Res Rev*. 2018;38(1):147-200. <https://doi.org/10.1002/med.21436>.
- [6] Macalino SJ, Gosu V, Hong S, Choi S. Role of computer-aided drug design in modern drug discovery. *Arch Pharm Res*. 2015;38(9):1686-1701. <https://doi.org/10.1007/s12272-015-0640-5>.

- [7] Stanzione F, Giangreco I, Cole JC. Use of molecular docking computational tools in drug discovery. *Prog Med Chem*. 2021;60:273-343. <https://doi.org/10.1016/bs.pmch.2021.01.004>.
- [8] Wong CF. Flexible receptor docking for drug discovery. *Expert Opin Drug Discov*. 2015;10(11):1189-1200. <https://doi.org/10.1517/17460441.2015.1078308>.
- [9] Amaro RE, Baudry J, Chodera J, Demir Ö, McCammon JA, Miao Y, Smith JC. Ensemble Docking in Drug Discovery. *Biophys J*. 2018;114(10):2271-2278. <https://doi.org/10.1016/j.bpj.2018.02.038>.
- [10] Van Drie JH. Monty Kier and the origin of the pharmacophore concept. *Internet Electron J Mol Des*. 2007;6(9): 271-279.
- [11] Wermuth CG, Robin Ganellin C, Lindberg P, Mitscher LA. Chapter 36 - Glossary of Terms Used in Medicinal Chemistry (IUPAC Recommendations 1997). In *Annual Reports in Medicinal Chemistry*, Bristol, J. A. Ed.; Vol. 33; Academic Press, 1998; pp 385-395.
- [12] Yang SY. Pharmacophore modeling and applications in drug discovery: challenges and recent advances. *Drug Discov Today*. 2010; 15 (11-12): 444-450. <https://doi.org/10.1016/j.drudis.2010.03.013>.
- [13] Lipinski CA. Drug-like properties and the causes of poor solubility and poor permeability. *J Pharmacol Toxicol Methods*. 2000; 44 (1): 235-249. [https://doi.org/10.1016/s1056-8719\(00\)00107-6](https://doi.org/10.1016/s1056-8719(00)00107-6).
- [14] Chen YC. Beware of docking! *Trends Pharmacol Sci*. 2015; 36 (2): 78-95. <https://doi.org/10.1016/j.tips.2014.12.001>.
- [15] de Ruyck J, Brysbaert G, Blossey R, Lensink MF. Molecular docking as a popular tool in drug design, an in silico travel. *Adv Appl Bioinform Chem*. 2016; 9: 1-11. <https://doi.org/10.2147/AABC.S105289>.
- [16] Bolcato G, Cuzzolin A, Bissaro M, Moro S, Sturlese M. Can We Still Trust Docking Results? An Extension of the Applicability of DockBench on PDBbind Database. *Int J Mol Sci*. 2019;20(14):3558. <https://doi.org/10.3390/ijms20143558>.
- [17] Plewczynski D, Łażniewski M, Augustyniak R, Ginalski K. Can we trust docking results? Evaluation of seven commonly used programs on PDBbind database. *J Comput Chem*. 2011;32(4):742-755. <https://doi.org/10.1002/jcc.21643>.
- [18] Cheng T, Li X, Li Y, Liu Z, Wang R. Comparative assessment of scoring functions on a diverse test set. *J Chem Inf Model*. 2009;49(4):1079-1093. <https://doi.org/10.1021/ci9000053>.
- [19] Erickson JA, Jalaie M, Robertson DH, Lewis RA, Vieth M. Lessons in molecular recognition: the effects of ligand and protein flexibility on molecular docking accuracy. *J Med Chem*. 2004;47(1):45-55. <https://doi.org/10.1021/jm030209y>.
- [20] Leach AR, Shoichet BK, Peishoff CE. Prediction of protein-ligand interactions. Docking and scoring: successes and gaps. *J Med Chem*. 2006;49(20):5851-5855. <https://doi.org/10.1021/jm060999m>.
- [21] Sutherland JJ, Nandigam RK, Erickson JA, Vieth M. Lessons in molecular recognition. 2. Assessing and improving cross-docking accuracy. *J Chem Inf Model*. 2007;47(6):2293-2302. <https://doi.org/10.1021/ci700253h>.
- [22] Friesner RA, Banks JL, Murphy RB, Halgren TA, Klicic JJ, Mainz DT, Repasky MP, Knoll EH, Shelley M, Perry JK, Shaw DE, Francis P, Shenkin PS. Glide: a new approach for rapid, accurate docking and scoring. 1. Method and assessment of docking accuracy. *J Med Chem*. 2004;47(7):1739-1749. <https://doi.org/10.1021/jm0306430>.
- [23] Halgren TA, Murphy RB, Friesner RA, Beard HS, Frye LL, Pollard WT, Banks JL. Glide: a new approach for rapid, accurate docking and scoring. 2. Enrichment factors in database screening. *J Med Chem*. 2004;47(7):1750-1759. <https://doi.org/10.1021/jm030644s>.
- [24] Friesner RA, Murphy RB, Repasky MP, Frye LL, Greenwood JR, Halgren TA, Sanschagrin PC, Mainz DT. Extra precision glide: docking and scoring incorporating a model of hydrophobic enclosure for protein-ligand complexes. *J Med Chem*. 2006;49(21):6177-6196. <https://doi.org/10.1021/jm051256o>.
- [25] Robaa D, Wagner T, Luise C, Carlino L, McMillan J, Flaig R, Schüle R, Jung M, Sippl W. Identification and Structure-Activity Relationship Studies of Small-Molecule Inhibitors of the Methyllysine Reader Protein Spindlin1. *ChemMedChem*. 2016;11(20):2327-2338. <https://doi.org/10.1002/cmdc.201600362>.
- [26] Molecular Operating Environment (MOE), 2019 Chemical Computing Group ULC, 1010 Sherbooke St. West, Suite #910, Montreal, QC, Canada, H3A 2R7.
- [27] Baell JB, Holloway GA. New substructure filters for removal of pan assay interference compounds (PAINS) from screening libraries and for their exclusion in bioassays. *J Med Chem*. 2010;53(7):2719-2740. <https://doi.org/10.1021/jm901137j>.
- [28] Walters WP, Murcko MA. Prediction of 'drug-likeness'. *Adv Drug Deliv Rev*. 2002;54(3):255-271. [https://doi.org/10.1016/s0169-409x\(02\)00003-0](https://doi.org/10.1016/s0169-409x(02)00003-0).

- [29] [https://www.asinex.com/screening-libraries-\(all-libraries\)](https://www.asinex.com/screening-libraries-(all-libraries)).
- [30] <https://chembridge.com/screening-compounds/lead-like-drug-like-compounds/#>.
- [31] <https://www.chemdiv.com/catalog/complete-list-of-compounds-libraries/>.
- [32] <https://enamine.net/compound-collections/screening-collection>.
- [33] Da C, Kireev D. Structural protein-ligand interaction fingerprints (SPLIF) for structure-based virtual screening: method and benchmark study. J Chem Inf Model. 2014;54(9):2555-2561. <https://doi.org/10.1021/ci500319f>.
- [34] Yuan H, Marmorstein R. Structural basis for sirtuin activity and inhibition. J Biol Chem. 2012 Dec 14;287(51):42428-35. <https://doi.org/10.1074/jbc.r112.372300>.
- [35] Hawkins PC, Skillman AG, Warren GL, Ellingson BA, Stahl MT. Conformer generation with OMEGA: algorithm and validation using high quality structures from the Protein Databank and Cambridge Structural Database. J Chem Inf Model. 2010;50(4):572-584. <https://doi.org/10.1021/ci100031x>.